Cumhuriyet Science Journal

e-ISSN: 2587-246X
ISSN: 2587-2680

Cumhuriyet Sci. J., 42(4) (2021) 965-976
http://dx.doi.org/10.17776/csj.811755

Effects of various heat treatments on microstructure and mechanical properties of investment cast Co-Cr-Mo implants

Kübra ÖZTÜRK [1, *], ***Onur ERTUĞRUL*** [2], ***Murat ÖZCAN*** [3]

[1] *Dokuz Eylül University, Department of Metallurgical and Materials Engineering, İzmir/TURKEY*
[2] *İzmir Katip Çelebi University, Department of Materials Science and Engineering, İzmir/TURKEY*
[3] *Eksen Hassas Dokum, İzmir/Turkey*

Abstract

In this study, the effects of various heat treatments (solutionizing, solutionizing + aging) on the microstructure and mechanical properties of the Co-Cr-Mo based hip implants produced by investment casting were investigated. The solution treatments were carried out at 1125°C, 1175°C and 1225°C for 3 hours under argon atmosphere. The aging treatments were carried at 850°C for 4 hours. The samples were examined under scanning electron microscope (SEM) and optical microscope (OM). Room temperature tensile tests and hardness tests were applied. The results showed that, the process of solutionizing at 1175°C and subsequent aging resulted in the formation of the smallest size precipitates with more homogeneous distribution in the interdendritic space of the as-cast structure compared to other treatments. According to tensile test results of the aged samples, as the solutionizing temperature increased to 1175°C both strength and elongation values increased. However, with the increase of solutionizing temperature to 1225°C, strength and elongation values decreased again. Solutionizing temperature of 1175°C gave the best microstructure-mechanical property relationship. Moreover, hardness values increased with the subsequent aging, yet do not change significantly with the solutionizing temperature.

Article info

History:
Received: 19.10.2020
Accepted: 13.12.2021

Keywords:
Solutionizing,
Aging,
Investment casting,
Hip implant,
Mechanical properties.

1. Introduction

Cobalt base alloys (Co–Cr–Mo), conforming to ASTM F-75 standard, are widely used in several medical applications such as knee and hip joint replacement, given their excellent biocompatibility, corrosion and wear resistance, combined with their good mechanical properties [1]. ASTM F-75 grade alloy is generally produced by investment casting method [2]. This method may lead to some defects in the as-cast position such as porosity, large grain size, hard precipitates in interdendritic zones, low ductility, low fatigue strength and inhomogeneties in carbide morphology and their size [2,3]. This is because the microstructures of the as-cast alloys, which indicate solidification segregation (interested to the formation of precipitates), considerably with the casting parameters (e.g., the melt temperature and cooling rate) [3, 4]. Several solutions to this problem have been suggested to decrease defect amount and to develop the mechanical properties such as ductility and strength of this alloy. However, the mechanical properties of these alloys can be improved by heat treatments by dissolving the wide carbide area and generate a more homogeneous microstructure [5]. Nevertheless, the mechanical properties can be improved with additional heat treatments by dissolving the large carbide network and produce a more homogeneous structure [6]. Lee et al. studied the effect of the addition of N on the microstructure and mechanical properties of the C-free Co-Cr-Mo alloys with various Cr contents. They revealed that Ni-free Co-Cr-Mo alloys with enriched Cr content up to 34 wt%, modified by N addition, are suitable for hip and knee joints that are produced on the basis of the casting process such as investment casting [7]. Their properties such as corrosion resistance, wear resistance, excellent biocompatibility, hardness of Co-Cr-Mo alloy depend mainly on the carbon content and the type of heat treatment applied [8]. The main strengthening mechanism of Co base alloys is the presence of second phase precipitates. The precipitation hardening performance of the alloy is closely related to the phase, size, amount, and distribution of precipitates in the metallic matrix [8,9].

*Corresponding author. *e-mail address: kubra94ozturk@gmail.com*

Gomez et al. investigated the effects of casting parameters such as pouring temperature on the microstructure of ASTM-F75 (Co-28%Cr-6%Mo) alloy [10]. They showed that mechanical properties can be optimized through controlling processing parameters. The microstructural study showed that pouring and preheating mold-temperatures affect the evolution of the microstructure during rapid cooling and various microstructures result in a large range of mechanical properties for the alloy ASTM-F75. The preheating mold temperature and the liquid temperature varied between 900, 1000, and 1410, and 1470°C, respectively. According to the results, optimum static strength and ductility were obtained when shrinkage microporosity decreased and the volume fraction of $M_{23}C_6$ type ''eutectic'' carbides precipitated at grain boundaries [10]. It is also found that the as-cast grain size is very sensitive to preheating mold and metal pouring temperatures. Moreover, the formation of ''eutectic'' carbides can be minimized by increasing the preheating mold and metal pouring temperatures [10,11].

Co-Cr-Mo alloys generally consist of a metastable γ (fcc) matrix and ε (hcp) martensite. The ε martensite is formed during quenching, plastic deformation, and isothermal heat treatment. [12]. The as-cast ASTM F-75 alloy consists of two primary phase microstructure: γ-face centered cubic (γ-fcc) phase and ε hexagonal close packed (ε-hcp). γ -face centered cubic (γ-fcc) phase which shows advanced elongation and ultimate tensile strength when temperature is high enough [12]. Another is ε-hcp phase which shows low elongation and brittle fracture on straining when temperature is low [4, 13]. Co-base alloys present a dentritic α-fcc metastable matrix due to tansformation of fcc→hcp so obtained precipitated formed in microstructured by $M_{23}C_6$ carbides, α or M_6C carbide phase σ phase both α and σ phases [13, 14]. Carbide precipitation at grain boundaries and interdendritic regions is the major strengthening mechanism in the as-cast condition. K. Yamanaka et al., studied the the effects of carbon on the relation between the microstructure and the mechanical properties of Ni-free Co–Cr–W-based cast alloys. Result of the study show that adding carbon to the alloys increased the amount of interdendritic precipitates that formed and changed the precipitation behavior [15].

The aim of the study is to investigate the effects of the heat treatment procedure and temperature on microstructure, tensile properties, and hardness of the investment-casted ASTM-F75 alloy. For the first set of samples, only solution treatment was applied at three different temperatures (1125, 1175 and 1225°C, respectively). Then, aging treatments were applied to the solutionized samples. The solution treatment was applied in order to provide fine and homogenously distributed grain structure, and also to dissolve some of the carbides in the post-casting structure. Additional aging treatments were applied in order to increase the strength and hardness values. With the optimum heat treatment, it is expected that the ductility of the final material will increase significantly compared to as–cast material.

2. Materials and Methods

2.1 Casting process

Cobalt based superalloy in accordance with the standard ASTM F-75 was used in this study which has Cr and Mo as main alloying elements and Ni, Fe, C, Mn and Si as trace elements. The casting is made by ASTM F-75 alloy ingot directly. The compositional limits of this alloy is shown in Table 1 and the spectrometer results of 7 samples produced in this study are listed in Table 2. There are three basic steps required for investment casting. These are wax-based mold preparation, dipping into ceramic slurry and shaping, and finally pouring molten metal into this mold. In the production step, firstly, the wax is melted at 72°C. It is mixed for homogenization. Then, it is injected into aluminum mould with the help of temperature and pressure. After visual and dimensional controls, wax models are being sticked to wax runner with the help of heat. Figure 1a represents the pattern creation step. After assemblying, tree is being coated with refractories. Refractories depend on quality requirements. Zircon, Alumina, various Alumina Silicates, Mahnezia can be used. Wax assemly is being coated with appropriate refractory and allowed to dry for every coating step. Next operations are wax removal with autoclave furnace and ceramic mold sinterring at 1000°C for 25 minutes. The aim of the sintering process is to prevent the thermal shock that may occur when the molten metal is spilled and to facilitate the sweep of the molten metal. While preheating the mould in furnace, the solid metal was placed in the induction furnace, and melted at 1560°C. Figure 1b demonstrates the melted metal in the furnace. The ceramic mold is connected to the furnace and the melt metal mold is poured. After 22 minutes, the casting ends as shown in Figure 1c. The mold is allowed to cool to room temperature as shown below in Figure 1d.

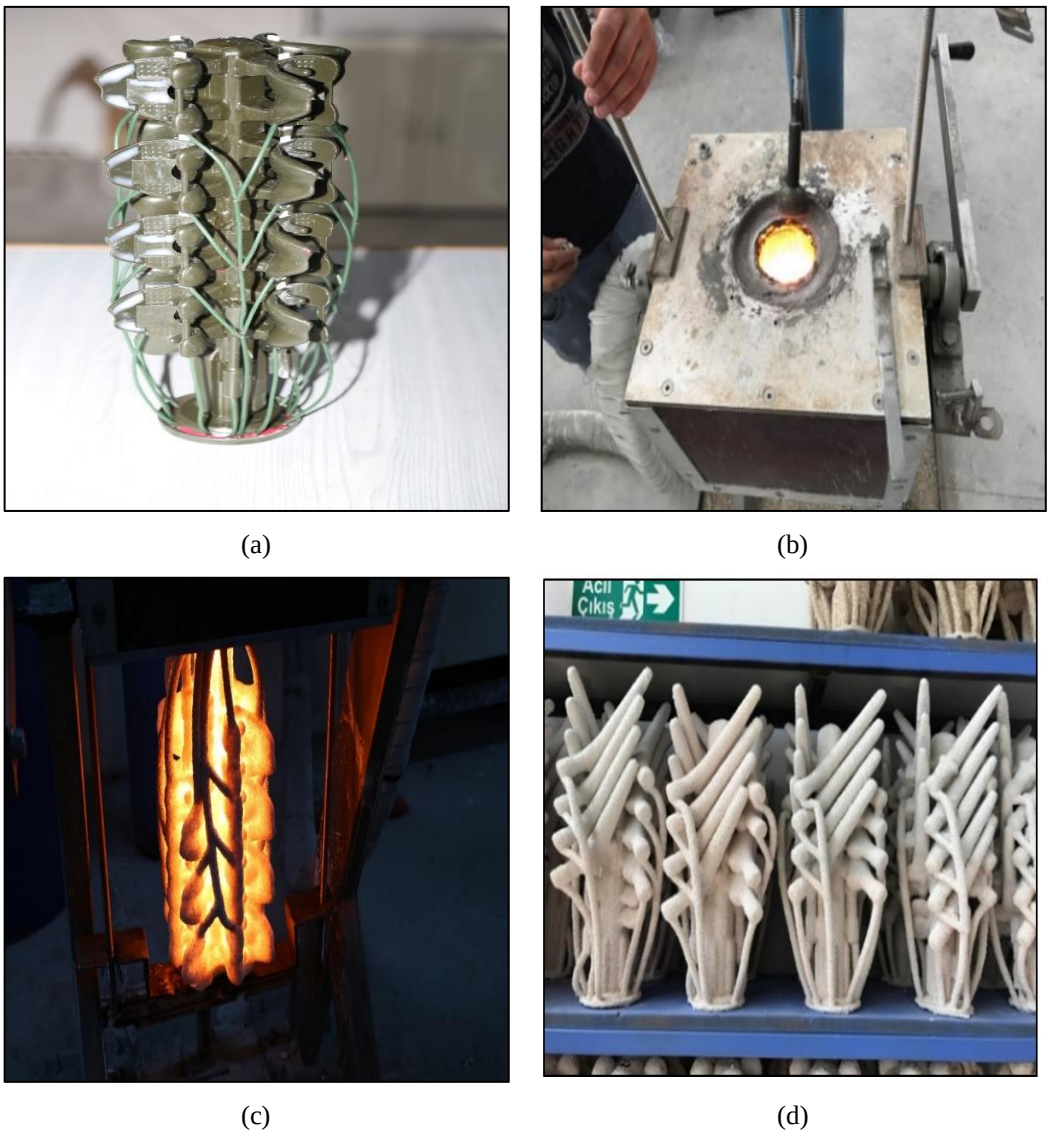

(a) (b)

(c) (d)

Figure 1. (a) Pattern creation, (b) Melting of ASTM F-75 alloy, (c) Pouring, (d) Cooling of mold

Table 1. The chemical composition of the ASTM F-75 alloy

Element (wt%)	Co	Cr	Mo	Ni	C	Si
ASTM F-75	Bal.	27-30	5-7	<0.50	<0.35	<1.0

Table 2. The spectrometry analysis results of the as-cast samples

Elements (%)	Cr	Mo	Ni	Fe	C	Mn	Si	Co
C1	28,17	5,34	0,23	0,28	0,22	0,59	0,32	64,84
C2	28,61	5,97	0,50	0,40	0,22	0,43	0,33	63,55
C3	27,31	5,83	0,22	0,27	0,27	0,59	0,30	65,21
C4	27,63	5,27	0,23	0,32	0,29	0,70	0,38	65,18
C5	27,78	5,87	0,42	0,39	0,25	0,36	0,59	64,34
C6	28,68	5,54	0,45	0,38	0,23	0,41	0,67	63,65
C7	28,48	5,35	0,23	0,32	0,24	0,59	0,38	64,41

2.2 Solution treatment and aging treatment processes

Six test samples were encoded as C1, C2, C3, C4, C5, and C6. Test samples were undergone to solution treatment (C1, C3, C5) and solution treatment + aging treatment (C2, C4, C6). One set of samples are shown in Figure 2a. The solution treatments were performed at 1125℃, 1175℃ and 1225℃ temperatures for 3 h, followed by quenching in water. The heat treatments were carried out in a high-temperature tube furnace under an inert gas atmosphere (Argon). The heat treatment setup is shown in Figure 2b. The aging treatment was performed at 850℃ for 4h. All samples were applied to solution treatment only whereas the C2, C4, C6 samples were subjected to only aging as shown in Table 3.

(a)

(b)

Figure 2. (a) Tensile test samples together with hardness samples of ASTM F-75 and (b) tubular furnace

Table 3. Sample coding and Experimental parameters used in the present study.

Sample Codes	Heat Treatment
C1	Solutionizing (1125℃)
C2	Solutionizing (1125℃) +Aging
C3	Solutionizing (1175℃)
C4	Solutionizing (1175℃) +Aging
C5	Solutionizing (1225℃)
C6	Solutionizing (1225℃) +Aging
C7	As-Cast (No heat treatment)

2.3 Microstructural study

The preparation of samples for optical microscopy (OM) and scanning electron microscopy (SEM) were carried out using conventional procedures such as grinding and polishing steps. The samples were first grinded with SiC grinding papers. Polish using diamond suspension (1 and 3 μm). Afterwards, the samples were thoroughly cleaned so as to remove any polishing residue. The sample surface was then etched to obtain examination of microstructure. Etching solution consist of 4 g Sodium Hydroxide, 100 ml water, 4 g potassium permanganate. This solution immersed over the surface for 25 seconds. Then the samples were cleaned by rinsing with ethanol. Then, the sample is placed on the optical microscope. The samples were examined also by SEM using a Carl Zeiss 300VP microscope which was operated at an acceleration voltage of 15 kV. Moreover, energy dispersive spectroscopy (EDS) techniques were employed to provide a more accurate characterization of the different precipitated phases, even though the EDS technique provides a semi-quantitative analysis.

2.4 Mechanical testing

Two tensile samples were cut from the produced hip implants. After solution treatment and aging heat treatment processes were applied, tensile samples are machined from the material in the desired orientation. The tensile test samples were 12.5 mm in gauge diameter (D), 10 mm in radius (R), 50 mm in gauge length (G), and 60 mm in reduced section (A). The tensile tests were applied using a crosshead speed of 1.5 mm/min by Zwick Z250 test machine. The technical drawing of the tensile test samples, which is taken from ASTM E8 standard, is given in Figure 3. Macrophotographs of a tensile test samples (a) before and (b) after the tests are given in Figure 4. In the

second mechanical testing phase, two different hardness tests were applied: Rockwell Hardness Test and Vickers Hardness Test (HV_1). A force of 9.8N was applied for an indentation time of 15 s in the microhardness test.

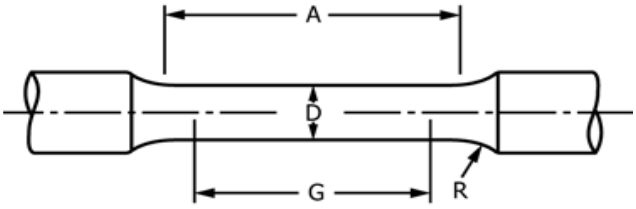

Figure 3. The technical drawing of a tensile test sample

(a) (b)

Figure 4. Macrophotographs of a tensile test sample (a)before and (b) after the test.

3. Results and Discussion

3.1 Microstructural evaluation by optical microscopy (OM)

3.1.1 Images of as-cast and solution treated samples

Co-base alloys exhibit a dendritic α-fcc metastable matrix due to the nature of the fcc→hcp transformation and a precipitate formed mainly by $M_{23}C_6$ carbides, and a lamellar phase formed by interlayed plates of $M_{23}C_6$ carbide and a phase [5]. $M_{23}C_6$ carbide initially present in the alloy tends to transform into M_6C carbide. According to microstructure of the various ASTM F-75, all samples showed Co grains with or without carbide precipitates depending on heat treatment conditions. These samples exhibited lameller type carbides on matrix structure. Figure 3 shows that the typical microstructure of as-cast condition with a cobalt matrix (FCC) containing primary lamellar and blocky carbides. Three different structure of the carbides in the as-cast microstructure can be determined. The "eutectic" carbide with lamellar morphology was formed at grain boundaries by interlayer plates of $M_{23}C_6$ carbide and a phase. These phases has not been clearly identified because it can be maybe σ or both α and σ phases. As-cast cobalt alloys the solidified microstructures consist of a predominantly FCC γ-dendritic structure which is accompanied by segregation, and second phase precipitates within the matrix and along the interdendritic regions [16]. In the case of as-cast alloys present highly inhomogeneous structure is expected to form with large-grained cored dendrites and Co-rich areas [16,17]. The microstructures observed by optical microscopy belong to as-cast condition are shown in Figure 5. This as-cast microstructure is the characteristic one as described above.

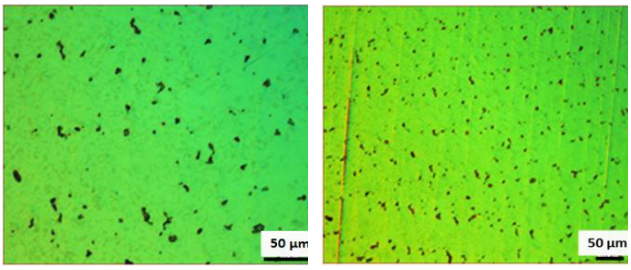

Figure 5. OM images belong to microstructure of the as-cast sample.

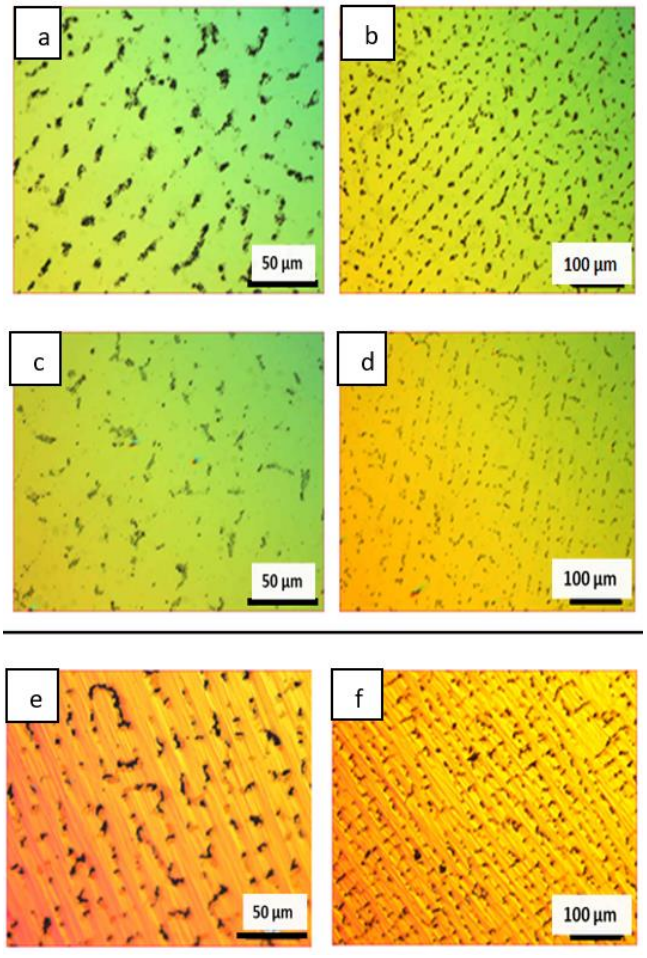

Figure 6. Microstructures of samples solutionized at (a-b) 1125°C (c-d); 1175°C, (e-f) 1225°C

Figure 6a and b show the microstructural evolution for solution treatment at 1125°C (Sample C1). There is a microstructural morphology change from lamellar to a more round-like form of $M_{23}C_6$ carbides as the solution treatment temperature increases. The chemical composition of these carbides corresponds to the $M_{23}C_6$ (M = Co, Cr and Mo) phase. As the $M_{23}C_6$ carbide suffers a spheroidization and sometimes could transform according to the $M_{23}C_6 \rightarrow M_6C$ reaction [8], it can also be noticed in Figure 6c-d and e-f respectively (Samples C3 and C5). It can be seen from these Figures that the morphology of the carbides changed, and the carbides have been shrunk with increasing solution treatment temperature.

3.1.2 Images of solution treated and aged samples

Carbide precipitation at grain boundaries and interdendritic regions is the major strengthening mechanism in the as-cast samples. Moreover, additional fine precipitate carbides are always beneficial in terms of strength and hardness increase in metallic materials.

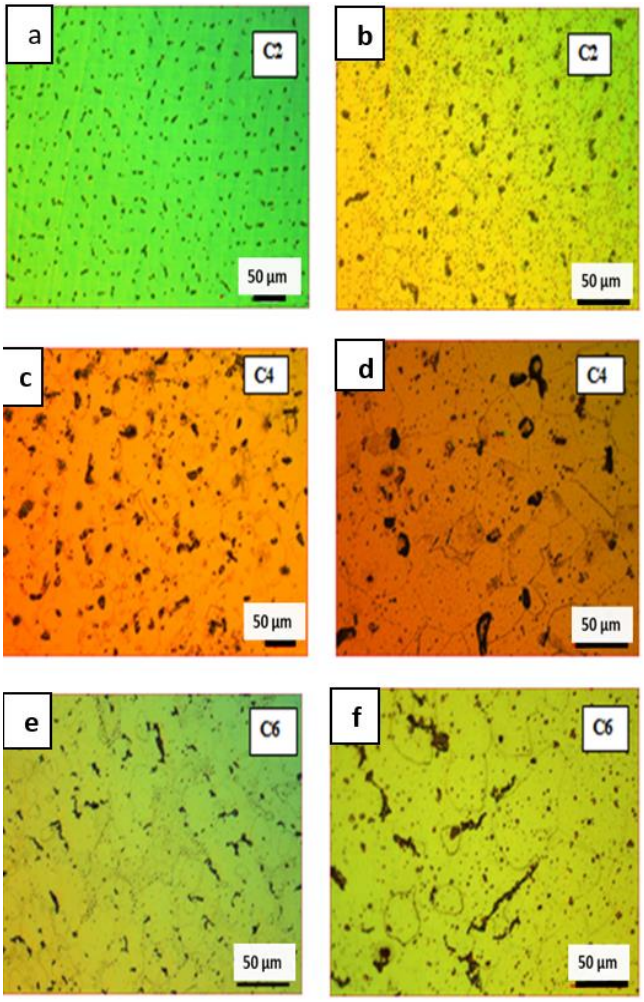

Figure 7. Microstructures of samples (a,b) solutionized at 1125°C and aged, (c,d) solitonized at 1175°C and aged and (e,f) solutionized at 1225°C and aged.

According to optical microscope images, matrix phase was observed with spheroidized $M_{23}C_6$ carbides in microstructures presented in Figure 7. Carbide precipitates are seen through the grain boundaries and also in the matrix structure. As a result, the strength of the material is increased significantly in C2 and C4 samples. In addition to that lamellar carbides, precipitations into the grains became more evident due to the aging process in all three conditions (C2, C4 and C6).

3.2 XRD analysis

Figure 8 shows the XRD patterns belong to the C7, C1 and C2 samples. Here, patterns belong to C1 and C2 samples were given as representative since the patterns for the samples C3-C4 and C5-C6 give similar results parallel to C1-C2. The pattern of the as-cast sample shows that both γ matrix phase with fcc crystal structure and ε phase with hcp structure are present. Also, the structure contains $M_{23}C_6$ type carbide phase. The structure of the as-solutionized condition contains γ and ε phases together, as seen in Figure 8b. After the subsequent aging process, the structure contains mainly a high intensity ε phase together with $M_{23}C_6$ type carbides and the matrix phase (γ).

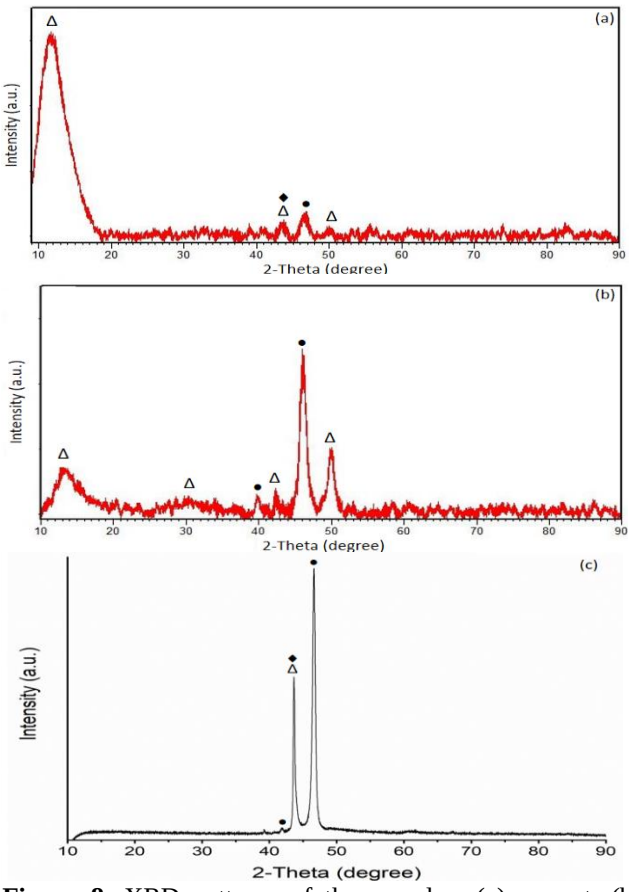

Figure 8. XRD patterns of the samples: (a) as-cast, (b) solutionized at 1125°C, (c) solutionized at 1125°C and aged (the symbols represent; Δ: fcc γ phase, •: hcp ε phase, ♦: $M_{23}C_6$ phase).

3.3 SEM study

3.3.1 As-cast and solution sreated samples

The as-cast microstructure corresponding to sample C7 is shown in Figure 9. The typical microstructure of as-cast alloy consists of a cobalt matrix (FCC) containing primary lamellar and carbides. It is showed a solid solution of Co as a matrix and also carbides as secondary phase. Figure 10a and b present the microstructure of the sample C1 showing the matrix and carbide phases together. The microstructure consists of a dendritic Co-rich fcc matrix and interdendritic precipitates. The SEM images show that the $M_{23}C_6$ carbide spheroidization tends to transformed M_6C carbide and also carbide size reduction, carbides homogeneously distributed and smaller in size when increased heat treatment temperature. These Figures show an electron backscattered SEM image of all samples, so bright area indicate that high atomic number and dark areas indicate that low atomic number of phase and also bright area representing solid matrix of phase; Co grains.

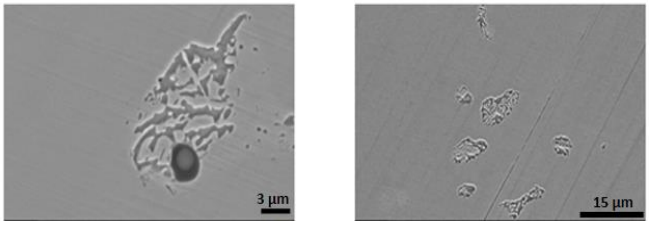

Figure 9. Microstructure of as-cast alloy.

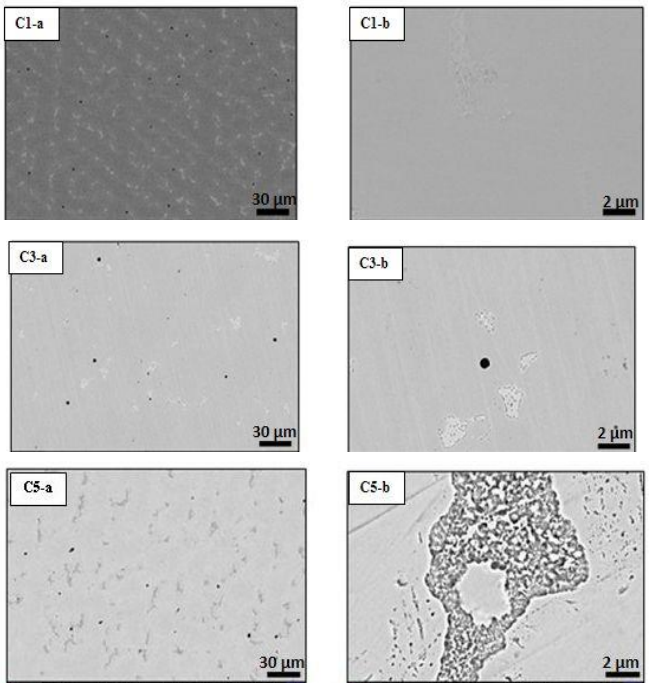

Figure 10. SEM images samples solutionized at C1 (a-b); 1125°C, C3 (a-b); 1175°C, C5 (a-b) 1225°C

Three areas were selected as shown in Figure 11 and Table 4. Selected area 1 show the Co-rich matrix composition with a 67.04 mass% of Co content. EDS Spot 1 analyse indicated that the secondary phase of Co-Cr-Mo phase occurs in the structure which is in accordance with the chemical composition of Co-Cr-Mo (ASTM F-75). EDS Spot 2 shows the higher concentration of Cr (46.96%), Mn (17.26%) and Si (30.51%) and also some amount of C. According to this result, Si-rich inclusions are within carbides in the middle of the interdendritic zones. Manganese and silicon are mainly in solution and are not segregated toward grain boundaries, and they are difficult to reveal. Co–Cr–Mo alloys with low and medium C content, as in this case, typically show very little grain boundary attack [10,18].

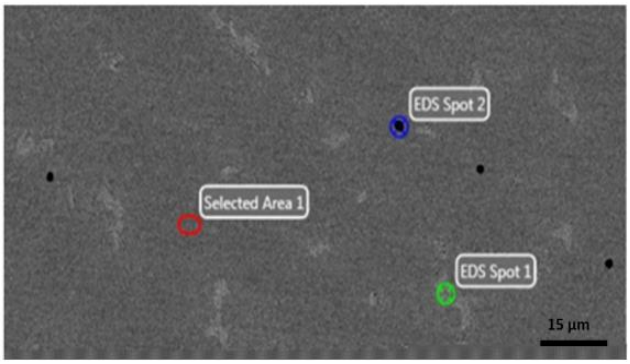

Figure 11. SEM micrograph corresponding to C1 and three regions were selected for analysis, selected area, EDS spot 1, EDS spot 2.

Table 4. Composition of elemental analysis for selected Area 1, EDS spot 1, EDS spot 2.

	Co	Cr	Mo	Mn	Si	C
Selected area 1	67,04	26.39	2.99	1,04	0.75	0.001
EDS Spot 1	46,51	34,86	13,37	1,05	1,50	1,67
EDS Spot 2	1,16	46,96	0,16	17,26	30,51	3,94

The EDS analysis corresponding to sample C3 belong to the areas spotted in Figure 12. Three area were selected as in the Table 5. From the obtained results, the higher concentration of Co rich matrix means that it is Co enriched and reaches the composition of 65.62 mass%. EDS Spot 2 and spot 3 analysis indicate that there is a secondary (eutectic) phase composed of Co, Cr and Mo elements as also found in the sample C1. From the result of Spot 1 analysis, it may be a Si-rich inclusion within the carbide in the middle of inter dendritic zones.

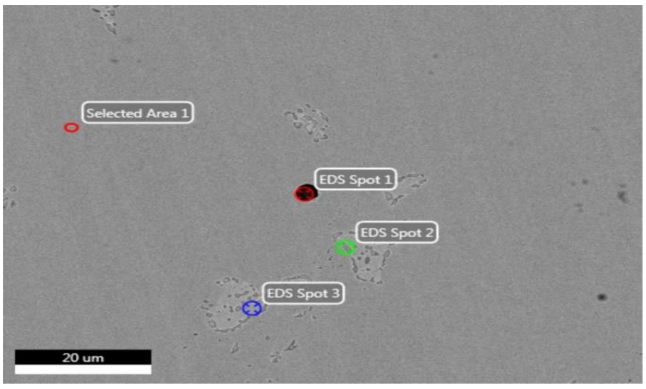

Figure 12. SEM micrograph corresponding to C3 and four regions were selected for analysis, EDS spot 1, EDS spot 2, EDS spot 3, selected area 1.

Table 5. Composition of elemental analysis for selected area 1, EDS spot 1, EDS spot 2, EDS spot 3.

	Co	Cr	Mo	Mn	Si	C
Selected area 1	65,62	27,08	3,89	1,03	0,92	0
EDS Spot 1	29,50	23,39	1,81	4,60	38,81	0
EDS Spot 2	57,45	27,43	10,22	1,09	1,81	0,33
EDS Spot 3	49,57	35,36	11,66	0,85	1,22	0

The EDS analysis corresponding to sample C5 are taken from the areas shown in the backscattered electron image of C5 (Figure 13). Three area were selected as in the Table 6. The higher concentration of Co found in bright area in the selected area 1, so it means that Co-rich matrix is Co enriched and reaches the composition of 82.27 wt.%. Here, all three EDS analysis indicate the famous intermetallic Co-Cr-Mo matrix phase with bright colour. Also, EDS spot 2 indicates a higher concentration of chromium compared to the other two which can be attributed to another secondary precipitation-like phase with dark colour.

Table 6. Composition of elemental analysis for selected area 1, EDS spot 1 and EDS spot 2.

	Co	Cr	Mo	Mn	Si	C
Selected area 1	82,27	14,99	1,94	0	0,80	0
EDS Spot 1	63,60	33,16	1,05	0,12	0,31	0
EDS Spot 2	79,62	15,68	3,65	0	0,87	0

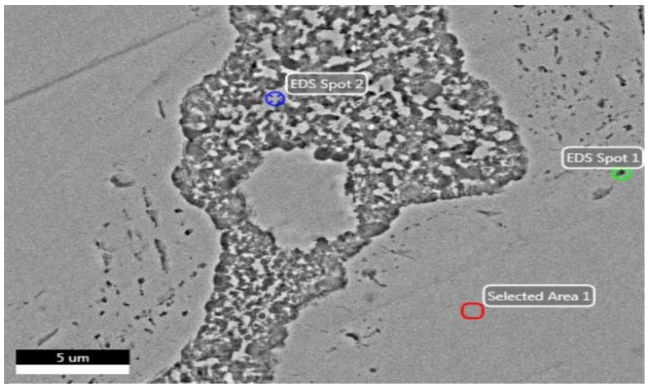

Figure 13. SEM micrograph corresponding to C5 and three regions were selected for analysing, EDS spot 1, EDS spot 2 and selected area 1.

3.3.2 Solution treated and aged samples

The typical microstructure of as cast-condition with a cobalt matrix (FCC) containing primary lamellar and blocky carbides. In general the as-cast microstructure is a Co-fcc dendritic matrix with the presence of a secondary phase, such as the $M_{23}C_6$ carbides precipitated at grain boundaries and at interdendritic zones. These precipitates are the main strengthening mechanism in this type of alloys [7]. Figure 14 represented that sample C2 has obvious $M_{23}C_6$ carbide and some possible M_6C carbide. The carbides in the shape of small dot like areas seen in C4 and C6 samples can be attributed to M_6C carbide presence.

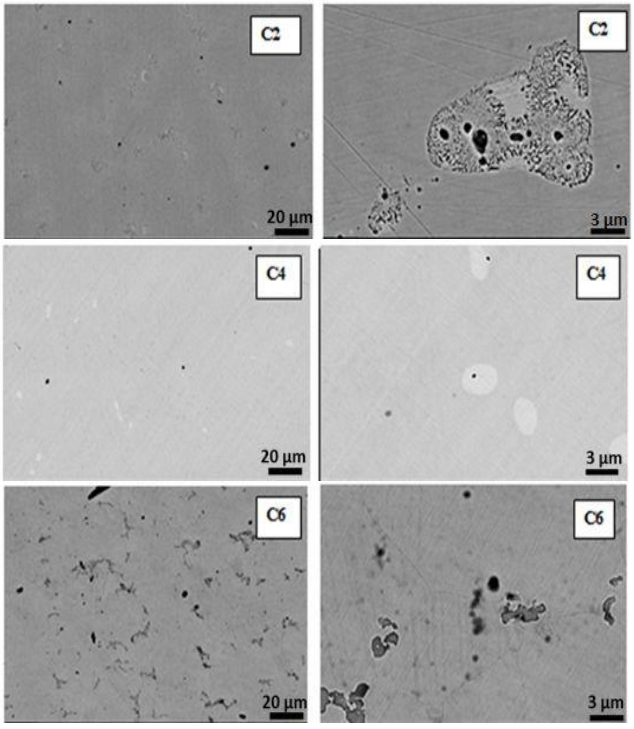

Figure 14. SEM micrograph of (a-b) C2, (c-d) C4 and (e-f) C6 samples.

C6 which is solution treated at 1225°C and aged, reveals lamellar type of carbides along are along within grain boundaries.

The EDS analysis taken from the areas shown in Figure 15 are belong to sample C2. Four different areas were selected as in the Table 7. Comments can easily be made that selected area 1 represents the matrix phase having the values of Co (82.80%) Cr (14.80%) and Mo (2.16%) which is in accordance with ASTM F-75 standard. Same result can be said for the selected area 2. Small black dots are detected in EDS spot 1 and EDS spot 2, which are mostly $M_{23}C_6$ type carbide. As the solution treatment progresses, the $M_{23}C_6$ carbide suffers a spheroidization and could transform according to the $M_{23}C_6 \rightarrow M_6C$ reaction [8].

Therefore, it should be noticed that some amount of these carbides could be transformed to M_6C type carbides.

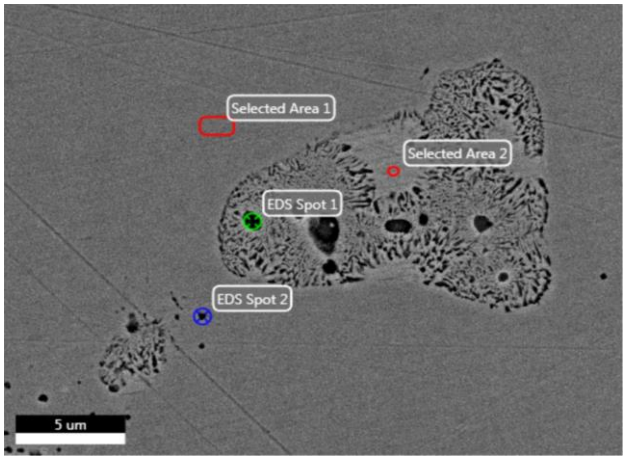

Figure 15. SEM micrograph corresponding to C2 and three regions were selected for analysis. (selected area 1, selected area 2, EDS spot 1, EDS spot 2)

Table 7. Composition of elemental analysis for selected area 1, selected area 2, EDS spot 1 and EDS spot 2.

	Co	Cr	Mo	Mn	Si	C
Selected area 1	82,80	14,80	2,16	0	0,84	0
EDS Spot 1	72,27	20,03	6,54	0	1,15	0
EDS Spot 2	71,19	21,32	6,26	0	1,10	0,07
EDS Spot 3	65,40	31,71	1,27	0	0,34	0

The EDS analysis taken from the areas shown in Figure 16 are belong to sample C4. Three areas were selected as in the Table 8. M_6C carbide phase detected in EDS spot 1. EDS spot 2 shows $M_{23}C_6$ carbide phase. It embraces EDS spot 1 which is M_6C carbide phase. Comments can easily be made that selected area 1 is the α phase so it evinces to higher value of Co (62.34%) Cr (28.74%) and Mo (4.85%) which is base matrix of ASTM F-75.

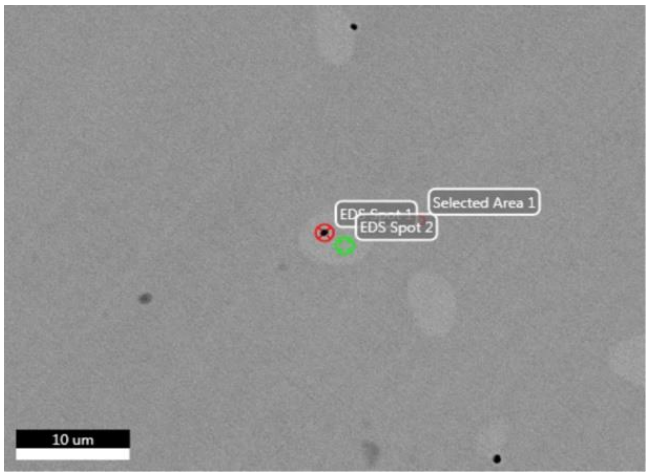

Figure 16. SEM micrograph corresponding to C4 and three regions were selected for analysis. (selected area 1, EDS spot 1, EDS spot 2)

Table 8. Composition of elemental analysis for selected area 1, EDS spot 1 and EDS spot 2.

	Co	Cr	Mo	Mn	Si	C
Selected area 1	62,34	28,74	4,85	0,96	0,94	0
EDS Spot 1	27,07	31,46	21,59	14,51	2,77	1,29
EDS Spot 2	49,79	34,63	11,40	1,07	1,21	0,21

The EDS analysis taken from the areas shown in Figure 17 are belong to sample C6. Four different areas were selected as in the Table 9. Different from C2 and C4 samples, there is one Cr-rich area (selected area 1) consists of higher amounts of Cr and C. The result confirms the presence of the $M_{23}C_6$ carbide phase.

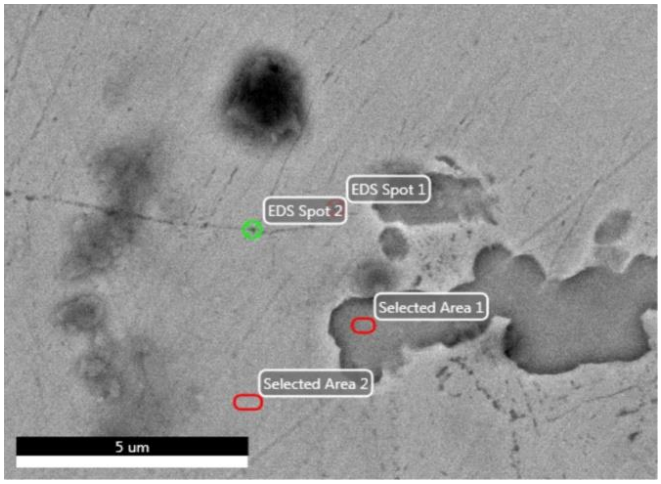

Figure 17. SEM micrograph corresponding to C6 and three regions were selected for analysis. (selected area 1, selected area 2, EDS spot 1, EDS spot 2)

Table 9. Composition of elemental analysis for selected area 1, EDS spot 1 and EDS spot 2.

	Co	Cr	Mo	Mn	Si	C
Selected area 1	18,21	67,87	7,64	0	0,74	5,44
Selected area 2	81,04	16,04	2,09	0	0,77	0
EDS Spot 1	80,65	16,42	2,14	0	0,78	0
EDS Spot 2	82,27	14,84	2,11	0	0,78	0

3.4 Mechanical test results

Table 10 shows mechanical test results of the samples. As can be seen from the table, solution treatment + aging conditions (C2, C4, C6) possess higher yield strength values than only solution treated samples (C1, C3, C5) and also higher than the as-cast condition. The solutionizing temperature of 1175℃ gives the highest yield strength values both solutionized and solutionized + aged conditions; 649 MPa and 683 MPa, respectively. When heat treatment temperature is increased to 1225℃, yield strength was decreased for C5 and C6. From result of these observation; the highest value of yield strength was obtained by aged samples, specially C4 at 1175℃ (683 MPa).

Table 10. Mechanical properties of the samples.

Sample Codes	Heat Treatment	YTS(Mpa)	UTS (MPa)	Elongation (%)	HV_1
ASTM F-75 *	-	450	665	8	-
C1	Solutionizing (1125°C)	521±23	742±37	9.3±0.5	355
C2	Solutionizing (1125°C) +Aging	613±21	763±62	8.4±0.1	365
C3	Solutionizing (1175°C)	649±56	826±56	9.05±0.65	350
C4	Solutionizing (1175°C) +Aging	683±23	829±58	9.75±0.25	364
C5	Solutionizing (1225°C)	521±19	716±8	8.6±0.2	351
C6	Solutionizing (1225°C) +Aging	635±65	738±20	8.5±0.5	362
C7	As-Cast	550±11	719±3	8.7±0.3	300

Table 10 also shows the effect of solutionizing temperature (1125℃, 1175°C, 1225°C) on tensile strength of for all heat treated conditions. As can be seen from the table 10, solution treatment + aging conditions (C2, C4, C6) possess higher yield strength values than only solution treated samples (C1, C3, C5) and also higher than as-cast condition. It is worth noting that, In the experiment carried out at 1175 degrees, a second phase was formed in the structure of the sample, which is soluble at high temperatures and has limited solubility at low temperatures. The precipitates of the microstructures interact with dislocations and tend to hinder their movement The presence of secondary phase grains increased the strength. We could observe fine precipitates in Fig. 7, in which grain size was a small size appears. As the temperature of the solution treatment was increased, the carbides reduced. The solutionizing temperature of 1175℃ gives the highest yield strength values both solutionized and solutionized + aged conditions; 826 MPa and 829 MPa, respectively. Owing to lamellar carbides that exist in the microstructure have led to the strength of the material increased significantly in C2 and C4 samples. As the heat treatment temperature was increased to 1225℃, tensile strength was decreased significantly for C5 and C6. As a result; the highest value of tensile strength was obtained by aged samples, specially C4 at 1175℃ (829 MPa).

When the elongation values are considered, the as–cast sample has the elongation value of 8.7 %. The sample which solution treated at 1125℃ temperature results similar value as as-cast sample. 1175℃ solutionized sample represents a lower elongation value of 9.05%. There has been decrease for 1225℃ solutionized sample which is the lowest elongation value for solution treated conditions. For aged samples (C2, C4, C6), C2 and C6 shows lower elongation values than all other conditions (8.4 and 8.5 % respectively). However, the C4 condition (both solutionized and aged at 1175℃) gives the best result of 9.75% elongation value which is remarkable among all samples.

The hardness values of the samples are given in the Figure 18. There is obvious increment value of hardness results ever then as-cast sample. Only heat treated samples showed the results of C1 (355 HV1),

C3 (350 HV1), C5 (351 HV1) values. It was clear from the results that aging temperature has an impact on hardness of the samples. The hardness values of aged samples is higher compared to that of solution-treated samples, aged samples gave higher hardness values than solutionized samples. Also, as the solutionizing temperature increases the hardness values stay constant with having C2 (365 HV_1), C4 (364 HV_1) and C6 (362 HV_1) hardness, respectively.

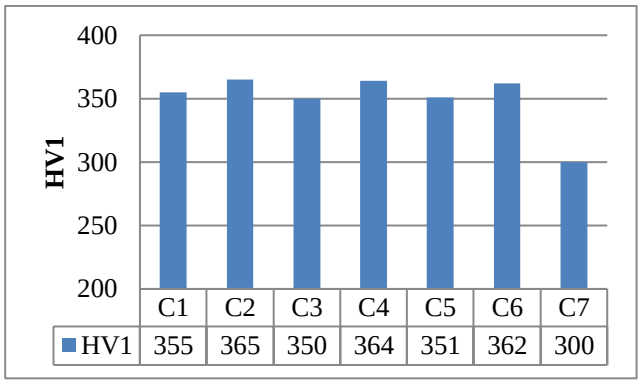

Figure 18. The hardness values of the samples

4. Conclusion

This paper presents the results of processing-microstructure and mechanical properties for ASTM F-75 alloy after applying both solution treatment and aging processes. The results obtained in this study can act as guidelines for tuning the microstructure of Co-Cr-based hip implants materials in order to increase their mechanical properties. The different phases present were identified using XRD and SEM EDX analysis. In all conditions, the microstructures agreed with the literature. As a result;

- The undissolved carbides of Cr, Mo, and Co have major effects on the microstructural and mechanical properties of the solution treated and aged samples. $M_{23}C_6$ type carbides and intermetallic phase were detected at grain boundaries and interdendritic zones. $M_{23}C_6$ carbides tend to spheroidize and also carbide size reduces. With increased heat treatment temperature, carbides are homogeneously distributed and begin to be smaller.
- The tensile tests showed that all heat treatments improved mechanical properties as both strength and ductility increased. For the as-solutionized samples, the best strength and ductility values have been obtained by solutionizing at 1175°C. Elongation values of solution treated and solution treated+aging samples exists in the range of 8.5 to 9.7 %.
- As the temperature increases to 1225°C, tensile strength and also yield strength decreased. Similar to this treatment, solutionizing at 1175°C and subsequent aging increased both yield, tensile strength and elongation. This treatment gives the highest mechanical properties as considerably high values have been obtained (e.g yield strength of 683 MPa, tensile strength of 829 MPa and an elongation of 9.75 %).
- Hardness values also increased with the subsequent aging process as hardness values are similar for three different solutionizing temperatures.
- It was demonstrated that samples from C4 alloy showed precipitates, much smaller size and with a more homogeneous distribution in the interdendritic space of the as-cast structure with respect to the other six alloys studied. Grain size is also effective in increasing the mechanical strength. This effect could be the result of the applied optimum heat treatment temperature (1175°C) and aging conditions when compared to other samples.

Acknowledgment

The authors would especially like to thank for the valuable support of the Mr. Önder ERTÜRKAN and the Ortopedya Implant A.Ş. company.

Conflicts of interest

The author declares that there is no conflict of interest.

References

[1] Giacchi J., V, Morando C.N., Fornaro O., Palacio H.A., Microstructural characterization of as-cast biocompatible Co–Cr–Mo alloys, *Materials Characterization*, 62(1) (2011) 53-61.

[2] Zangeneh S.H., Lashgari H.R., Saghafİ M., Karshenas M., Effect of isothermal aging on the microstructural evolution of Co–Cr–Mo–C alloy, *Materials Science and Engineering*, 527(24-25) (2010) 6494–6500.

[3] Montero O.C., Talavera M., Lopez H., Effect of alloy preheating on the mechanical properties of as-cast CoCrMoC alloys, *Metallurgical Materials Transactions*, 30 (1999) 611–20.

[4] Dobbs H.S., Robertson J.L.M., Heat treatment of cast Co–Cr–Mo for orthopaedic implant use, *J Mater Sci*., 18 (1983) 391–401.

[5] Yamanaka K., Mori M., Chiba A., Influence of carbon addition on mechanical properties and microstructures of Ni-free Co–28Cr–9 W–1Si–C alloys subjected to thermomechanical processing, *J. Mech. Behav. Biomed. Mater*., 37 (2014) 274–85.

[6] Youdelis W.V., Kwon O., Carbide phases in cobalt of subsize tensile test specimens and the traditional base superalloy: Role of nucleation entropy in refine- method of measuring % elongation to fracture by joinment, *Metal Sci*., 17(8) (1983) 379–384.

[7] Lee S.H., Nomura N., Chiba A., Significant improvement in mechanical properties of biomedical Co-Cr-Mo alloys with combination of N addition and Cr enrichment, *Mater. Trans*., 49(2) (2008) 260–264.

[8] Yamanaka K., Mori M., Chiba A., Assessment of precipitation behavior in dental castings of a Co–Cr–Mo alloy, *Mechanical Behavior Biomedical Materials*, 50 (2015) 268–27.

[9] Li S.J., Niinomi M., Akahori T., Kasuga T., Yang R., Hao Y.O., Fatigue characteristics of bioactive glass-ceramic-coated Ti–29Nb–13Ta–4.6Zr for biomedical application, *Biomaterials*, 25(17) (2004) 3369-3378.

[10] Gomez M., Mancha H., Salinas A., Rodryguez J.L., Escobedo J., Castro M., Mendez M., Relationship between microstructure and ductility of investment cast ASTM F-75 implant alloy, *Journal of Biomedical Materials Research*, 34(2) (1997), 157–163.

[11] Sims C.T, Hagel W., Stoloff N., The Superalloys II: High temperature materials for aerospace and industrial power, 2nd ed. New York: Wiley & Sons, (1987).

[12] Ramírez V.L.E., Castro R.M., Herrera T.M., García L.C.V., Almanza C.E., Cooling rate and carbon content effect on the fraction of secondary phases precipitate in as-cast microstructure of ASTM F75 alloy, *J Material Process Technology*, 209(4) (2009) 1681–1687.

[13] Rosenthal R., Cardoso B.R., Bott I.S., Paranhos R.P.R., Carvalho E.A., Phase characterization in as-cast F-75 Co-Cr-Mo-C alloy, *J. Mater. Sci*., 45(15) (2010) 4021–4028.

[14] Yamanaka K., Mori M., Sato K., Chiba A., Characterisation of nanoscale carbide precipitation in as-cast Co–Cr–W-based dental alloys, *J. Mater. Chem. B.*, 4(10) (2016) 1778–1786.

[15] Yamanaka K., Mori M., Chiba A., Effects of carbon concentration on microstructure and mechanical properties of as-cast nickel-free Co–28Cr–9W-based dental alloys, *Mater. Sci. Eng*., 40(7) (2014) 127–134.

[16] Ledesma A.L.R., Lopez H.F., Islas J.A.J., Evaluation of chill cast Co-Cr alloys for biomedical applications, *Metals*, 6(8) (2016) 188.

[17] Salam S., Hou P.Y., Zhang Y.D., Zhang X.H., Wang H.F., Zhang C., Yang Z.G., Microstructural modelling solution for complex Co based alloys and coatings, *Surf. Coat. Technol*., 236 (2013**)** 510–517.

[18] Herrera T.M., Espinoza A., Méndez J., Castro M., López J., Rendón J., Effect of C content on the mechanical properties of solution treated as-cast ASTM F75 alloys, *J Mater Sci Mater Med*., 16(7) (2005) 607–11.